Development of a mouse model of human coronavirus NL63 (HCoV-NL63) infection

J.K. Bentley, M. Han, C. Stroupe, H. Breckenridge, A. Mello, S. Jazaeri, A. Goldsmith, S.C. Baker, C.N. Lumeng, and M.B. Hershenson
Dept. of Pediatrics, University of Michigan Medical School, Ann Arbor, Michigan
Dept. of Microbiology and Immunology, Loyola University, Chicago

University of Michigan Medical School

ABSTRACT

Introduction: The SARS CoV2 pandemic has produced morbidity and mortality worldwide depending on age, body mass index, cardiovascular disease and other factors. Of the human CoVs, SARS-CoV2 and HCoV-NL63 bind ACE2. HCoV-NL63 causes upper respiratory tract infections in children, pneumonia in the elderly, and even Kawasaki disease in children. **Hypothesis**: HCoV-NL63 produces lung inflammation in mice expressing the human ACE2 protein. **Methods:** HCoV-NL63 (ATCC) was propagated in Caco-2 cells. Virus cytopathic effect in Vero cells at 48 h infection was determined by $TCID_{50}$. B6.Cg-Tg(K18-ACE2)2Prlmn mice (JAX Labs) express the human ACE2 protein in epithelial cells using the keratin 18 promoter. Eight-10 week-old K18-hACE2 or C57BL6/J mice were infected with 50 µL (100,000 $TCID_{50}$) HCoV-NL63 or sham intranasally and euthanized at 2, 4, and 7 days post-treatment. Mouse lungs were assessed for histology, IFN and cytokine mRNAs, ACE2, viral RNA and HCoV-NL63 proteins (nucleoprotein, Nsp3 and Nsp4). Primers from the HCoV-NL63 sequence (NC_005831.2) were used to measure vRNA by qPCR. Polyclonal antibodies to Nsp3 and 4 were (Chen *et al, J Virol* 2007) used with antibodies to human ACE2 (InVitrogen), HCoV-NL63 nucleoprotein (clone 2D5, Eurofins) for immunohistochemistry. **Results**: HCoV-NL63 cytopathic effects in Vero cells colocalized with viral nucleoprotein. Virus propagated in K18-hACE2 but not C57BL6/J mice. vRNA levels plateaued 4 days after infection and were detectable 7 days after infection. Lung mRNA expression of IFN-α, IFN-β, IFN-λ, CXCL1 and IL-6 were significantly increased 48 h after infection in HCoV-NL63-treated K18-hACE2 but not C57BL6/J mice (*N*=3, p<0.05, Kruskal-Wallis test). Mouse lung had bronchovascular and peribronchial inflammation evident 7 days after infection. Nucleoprotein was found on the apical surface of airway epithelial cells of HCoV-NL63- but not sham-infected K18-hACE2 mice, and Nsp3 and Nsp4 were found in the basal cytoplasm of airway epithelial cells. **Conclusion:** Human coronavirus NL63 infects K18-ACE2 mice with an airway inflammatory response. Viral replication is evident. This model may be used to study HCoV-NL63-induced exacerbation of allergic airways disease; the effect of allergy, obesity and aging on human coronavirus infection, and possible cross-immunity between HCoV-NL63 and other respiratory viruses

INTRODUCTION

SARS-CoV2 is one of a family of seven coronaviruses which cause respiratory infections in humans. HCoV-NL63 carries many similarities to SARS-CoV2. It shares the same receptor (angiotensin-converting enzyme 2, ACE2). NL63 has been sequenced in its entirety (1), allowing the development of a viral copy number assay that along with titration for cytopathic effect can be used to quantitate the virus. Antibodies have been developed to the viral nucleoprotein (2) as well as nonstructural proteins expressed during its replicative cycle intracellularly (3) that allow its detection in cells and tissues.

We aim to establish an animal model of HCoV-NL63 using a transgenic mouse that expresses the human ACE2 receptor (4). This model will be used to determine cellular mechanisms of coronavirus pathogenesis and test therapeutic interventions.

METHODS

Virus propagation and titer. HCoV-NL63 (BEI Resources) was grown in CaCo-2 or Vero cells (5,6). Initial stocks were prepared by freezing flasks at -70ºC, thawing, and centrifugation for 10 min at 5000 x *g* to remove particles. Cleared CaCo-2 cell supernatants from large scale preparations was concentrated by Centricon ultrafiltration filter unit with a 100 kDa cutoff. Titer was determined on 96 well plates of Vero cells at 80% confluence. Cytopathic effect visible after 48 h at 33ºC was verified using immuno- fluorescence to estimate a tissue culture infectious dose (TCID50) by the method of Spearman-Karber.

Viral detection. To detect HCoV-NL63 in cells and lung tissue, antibodies to the HCoV-NL63 N-protein (Eurofins) and nsp3 and -4 were used. Purified primary antibodies were labeled for immunofluorescence using AlexaFluor dye-conjugated N-hydroxy succinimidyl esters.

Measurement of HCoV-NL63 infectivity: quantitative polymerase chain reaction (qPCR). To measure lung viral RNA, total RNA was prepared using Trizol (InVitrogen, Carlsbad, CA) extraction and RNAeasy purification (Qiagen). First strand cDNA was prepared using the SuperScript IV system (Applied Biosystems). RNA was detected using an adaptation of previously described methods (7) to produce an 86 base pair product on qPCR using Sybr Green (Applied Biosystems) extending from bases 24-106 of the GenBank sequence NC_005831.2. A plasmid containing bases 1-540 of the sequence was used as a copy number standard (GenScript, Piscataway, NJ).

Genotyping mice. Mice (B6.Cg-Tg(K18-ACE2)2Prlmn/J, JAX Labs, Bar Harbor, ME) were genotyped using the recommended TaqMan qPCR assay on genomic DNA (8) and confirmed by RNA expression of human ACE2 as assessed by RT-qPCR.

Infection of mice. Adult K18-ACE2 mice were inoculated intranasally with 1 x 10^5 TCID50 equivalents NL63 or CaCO-2 cell sham. At 2, 4, and 7 days mice were harvested for lung histology or RNA isolation.

H*istology and immunofluorescence.* After sacrifice, mouse right arteries were perfused with PBS + 5mM EDTA, the left lung tied off and excised for RNA. The tracheas were intubated and perfused with formalin, and the lungs processed for paraffin sectioning. Sections were stained with hematoxylin and eosin (H&E) or immunofluorescence as described in the Figure legends.

Lung mRNA expression was estimated by qPCR as described in the Figure legends.

METHODS AND RESULTS

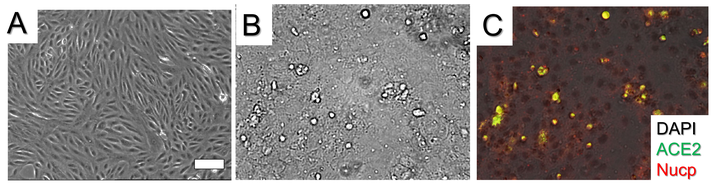

Figure 1 HCoV-NL63 produces cytopathic effects on Vero cells. In A, cells are treated with a sham cell extract for 48h. Cells remain a monolayer. The white scale bar is 50 microns. In B, cells are treated with 100,000 TCID50 units of NL63. Cells tend to round up and express granules at 48h. In C, the cells have been fixed and subsequently permeabilized with Tris-buffered saline containing 0.1% triton-x100 and 0.05% Tween 20. Anti human ACE2 (Invitrogen) was labeled with AlexaFluor 488, and anti NL63 nucleoprotein (Nucp) was labeled with AlexaFluor 555. After purification, these antibodies were combined with 4′,6-diamidino-2-phenylindole (DAPI) to stain cells. Nuclear DAPI staining is shown in an underlayer in black, while ACE2 is shown in green and Nucp staiing in red. The green ACE2 and red Nucp colocalize in infected cells as orange to yellow.

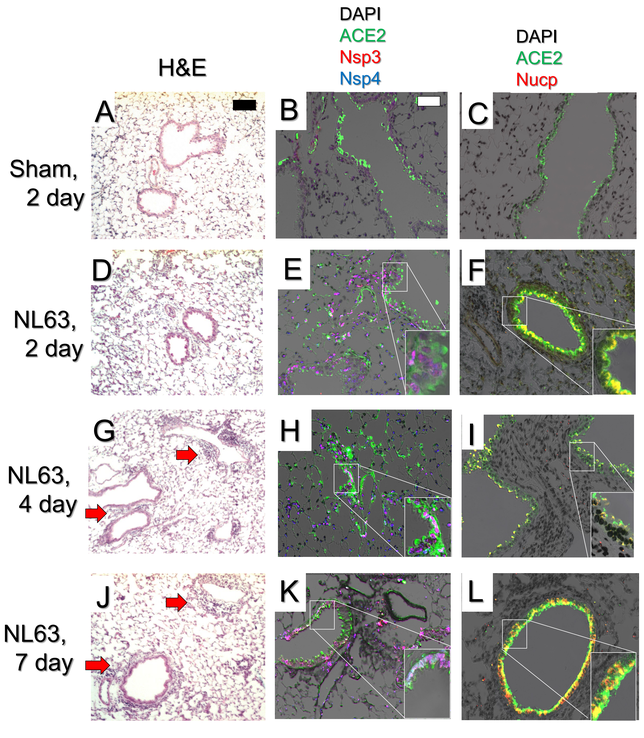

Figure 2 Sections of mouse lung demonstrated bronchovascular and peribronchial inflammation that were most evident 4-7 days after infection. Sections A-C were from sham treated mice harvested at 48 h treatment; D-F sections were also harvested at 48h but from 100,000 TCID50 unit infected mice; G-I at 4 days post treatment; and J-L at 7 days post treatment. Panel A and the first for each series is an H&E stain showing no inflammation in the sham. Areas of increased infiltration are shown with red arrows. The black scale bar is 100 microns. Panels B and C are stained for ACE2 in green with the white bar equivalent to 50 microns. There is no sham staining for nsp3 (red) or nesp4 (blue) (panel B) or nucp (red) (panel C). The white bar is 50 microns. At 48 h there is a diffuse cellular staining in the peribronchiolar and perivascular regions of the H&E stain (panel D) as well as red nsp 3 and blue nsp4 colocalization as purple-magenta (panel E). The inset (2x the original magnification of the original outlined area) shows this is diffusely cytoplasmic in the epithelium. Nucp and ACE2 colocalization in the epithelium is found at 48 h (panel F). By 4 and 7 days there a massive white cell infiltration as evidenced by blue nuclei in panels G as well as high epithelia colocalization of nsp3, 4 and 7. By day 7 the inflammation is largely peribronchiolar.

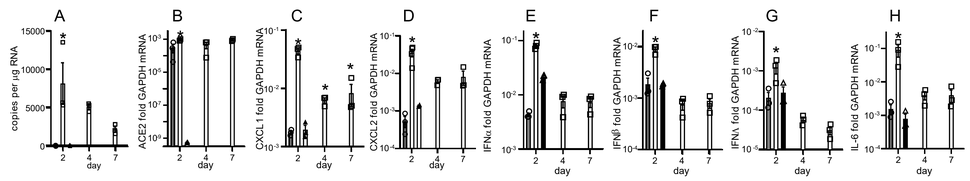

Figure 3. HCoV NL63 propagates in mouse lung and increases expression of cytokine mRNA. Mice were treated as described in the Figures with sham (circles and gray bars) or NL63 and lung mRNA purified for RT-qPCR on the indicated days from 3 mice per group shown. Primers used for NL63 copy number qPCR were described in Methods. Primers for human ACE2 were derived from NIH BLAST, as were mouse cytokine primers (9,10). Virus propagated in K18-hACE2 (squares and open bars) but not wild type mice (triangles and black bars, panel A), while there was no significant effect on ACE2 (panel B). NL63 treatment caused lung mRNA expression of CXCL1 (panel C), CXCL2 (panel D), IFN-α (panel E), IFN-Aβ (panel F), IFN-λ (panel G), and IL-6 (panel H) to be significantly (*) increased 48 h after infection in HCoV-NL63-treated K18-hACE2 but not C57BL6/J mice (*N*=3, p<0.05, Kruskal-Wallis test.

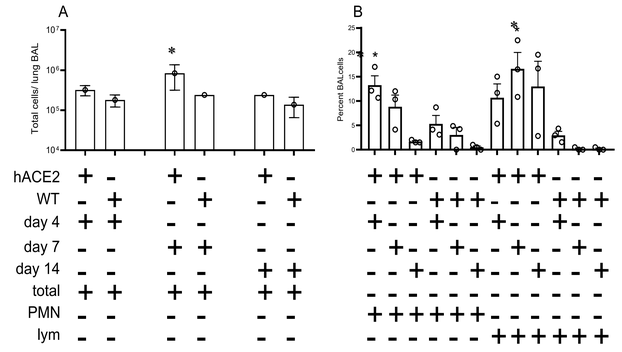

Figure 4. HCoV NL63 increases leukocyte and lymphocyte infiltration into the lung. Mice were treated as described in the Figures with sham or 100,000 TCID50 units of NL63. Lung BAL was performed on 3 mice per group shown at days 4, 7, and 14 post-treatment. Human ACE2-expressing mice (hACE2) had significantly more total cells than wild type (WT) mice at day 7 (*N*=3, p<0.05, ANOVA, panel A), significantly more neutrophils (PMN) at day 4, and significantly more lymphocytes at day 7.

SUMMARY AND CONCLUSIONS

Human coronavirus NL63 infects K18-ACE2 mice and induces an airway inflammatory response.

Viral replication is evidenced by vRNA levels, interferon mRNA expression and production of non-structural viral proteins.

This model may be used to study HCoV-NL63-induced exacerbation of allergic airways disease; the effect of allergy, obesity and aging on human coronavirus infection, and possible cross-immunity between HCoV-NL63 and other respiratory viruses.

REFERENCES

1. van der Hoek L, Pyrc K, Jebbink MF, Vermeulen-Oost W, Berkhout RJ, Wolthers KC, Wertheim-van Dillen PM, Kaandorp J, Spaargaren J, and Berkhout B. (2004) *Nat Med.* 10(4):368-73.
2. Sastre, P., Dijkman, R., Camuñas, A., Ruiz, T., Jebbink, M. F., van der Hoek, L., Vela, C., and Rueda, P. (2011). *Clin. Vac. Immunol.* 18(1), 113–118.
3. Chen, Z., Wang, Y., Ratia, K., Mesecar, A. D., Wilkinson, K. D., and Baker, S. C. (2007). *J. Virol.* 81(11), 6007–6018.
4. Oladunni FS, Park JG, Pino PA, Gonzalez O, Akhter A, Allué-Guardia A, Olmo-Fontánez A, Gautam S, Garcia-Vilanova A, Ye C, Chiem K, Headley C, Dwivedi V, Parodi LM, Alfson KJ, Staples HM, Schami A, Garcia JI, Whigham A, Platt RN 2nd, Gazi M, Martinez J, Chuba C, Earley S, Rodriguez OH, Mdaki SD, Kavelish KN, Escalona R, Hallam CRA, Christie C, Patterson JL, Anderson TJC, Carrion R Jr, Dick EJ Jr, Hall-Ursone S, Schlesinger LS, Alvarez X, Kaushal D, Giavedoni LD, Turner J, Martinez-Sobrido L, and Torrelles JB. (2020) *Nat Commun.* 11(1):6122.
5. Herzog P, Drosten C, and Müller MA. (2008) *Virol J.* 5:138.
6. Schildgen O, Jebbink MF, de Vries M, Pyrc K, Dijkman R, Simon A, Müller A, Kupfer B, and van der Hoek L. (2006) *J Virol Methods*.138(1-2):207-10.
7. Donaldson EF, Yount B, Sims AC, Burkett S, Pickles RJ, and Baric RS. (2008) *J Virol* 82: 11948-11957
8. McCray PB Jr, Pewe L, Wohlford-Lenane C, Hickey M, Manzel L, Shi L, Netland J; Jia HP, Halabi C, Sigmund CD, Meyerholz DK, Kirby P, Look DC, and Perlman S. (2007) *J Virol* 81(2):813-21.
9. Han, M., Bentley, J. K., Rajput, C., Lei, J., Ishikawa, T., Jarman, C. R., Lee, J., Goldsmith, A. M., Jackson, W. T., Hoenerhoff, M. J., Lewis, T. C., and Hershenson, M. B. (2019). *Mucosal immunology*, *12*(4), 958–968.
10. Han M, Hong JY, Jaipalli S, Rajput C, Lei J, Hinde JL, Chen Q, Hershenson NM, Bentley JK, and Hershenson MB. (2017) *Am J Respir Cell Mol Biol.* 56(2):242-251.